ADVANCED HEALTHCARE MATERIALS

www.advhealthmat.de

Fabrication of Calcium Phosphate-Based Nanocomposites Incorporating DNA Origami, Gold Nanorods, and Anticancer Drugs for Biomedical Applications

Hongbo Zhang, Xiangmeng Qu, Hong Chen, Haixin Kong, Ruihua Ding, Dong Chen, Xu Zhang, Hao Pei, Hélder A. Santos, Mingtan Hai, and David A. Weitz**

DNA origami is designed by folding DNA strands at the nanoscale with arbitrary control. Due to its inherent biological nature, DNA origami is used in drug delivery for enhancement of synergism and multidrug resistance inhibition, cancer diagnosis, and many other biomedical applications, where it shows great potential. However, the inherent instability and low payload capacity of DNA origami restrict its biomedical applications. Here, this paper reports the fabrication of an advanced biocompatible nano-in-nanocomposite, which protects DNA origami from degradation and facilities drug loading. The DNA origami, gold nanorods, and molecular targeted drugs are co-incorporated into pH responsive calcium phosphate [$Ca_3(PO_4)_2$] nanoparticles. Subsequently, a thin layer of phospholipid is coated onto the $Ca_3(PO_4)_2$ nanoparticle to offer better biocompatibility. The fabricated nanocomposite shows high drug loading capacity, good biocompatibility, and a photothermal and pH-responsive payload release profile and it fully protects DNA origami from degradation. The codelivery of DNA origami with cancer drugs synergistically induces cancer cell apoptosis, reduces the multidrug resistance, and enhances the targeted killing efficiency toward human epidermal growth factor receptor 2 positive cells. This nanocomposite is foreseen to open new horizons for a variety of clinical and biomedical applications.

1. Introduction

Recent advances in nanotechnology have revolutionary impact on modern drug delivery and cancer treatment.[1] DNA origami technology is a breakthrough in nanofabrication, which greatly simplifies the programmable design of 2D and 3D objects at the nanoscale.[1b,2] Through self-assembly of a long single-stranded scaffold with a multitude of short DNA strands, DNA origami can be tailored into a desired nanostructure within a few hours.[1b] DNA origami is highlighted in many biomedical applications.[3] Its sequence-specific property enables the DNA origami to target certain cellular receptors and achieve targeted drug delivery;[4] it also enables specific and sensitive detection of nucleic acids, metal ions, and proteins.[5] DNA origami is also biocompatible and biodegradable, and until now no obvious toxicity has been observed in its drug delivery applications. However, the instability, low payload capacity, and possible innate immune

Prof. H. Zhang, Dr. X. Qu, H. Kong,[+] Prof. M. Hai
Beijing Key Laboratory of Function Materials for Molecule and Structure Construction
School of Materials Science and Engineering
University of Science and Technology Beijing
Beijing 100083, P. R. China
E-mail: mingtanhai@ater.ustb.edu.cn, mhai@seas.harvard.edu

Prof. H. Zhang, Dr. X. Qu, R. Ding, Prof. D. Chen, Dr. X. Zhang,[++]
Prof. M. Hai, Prof. D. Weitz
Harvard John A. Paulson School of Engineering and Applied Science
Harvard University
Cambridge, MA 02138, USA
E-mail: weitz@seas.harvard.edu

[+]Present address: Cambridge International Curriculum Centre of Beijing Normal University, Beijing 100009, P. R. China

[++]Present address: Verschuren Centre, Cape Breton University, 1250 Grand Lake Road, Sydney, NS B1P 6L2, Canada

Prof. H. Zhang
Department of Pharmaceutical Sciences Laboratory
Åbo Akademi University
Turku 20520, Finland

Dr. X. Qu, Prof. H. Pei
School of Chemistry and Molecular Engineering
East China Normal University
500 Dongchuan Road, Shanghai 200241, P. R. China

Prof. H. Chen
Pen-Tung Sah Institute of Micro-Nano Science and Technology of Xiamen University
Xiamen University
Xiamen, Fujian Province 361005, P. R. China

Prof. H. A. Santos
Division of Pharmaceutical Chemistry and Technology
University of Helsinki
Helsinki FI-00014, Finland

DOI: 10.1002/adhm.201700664

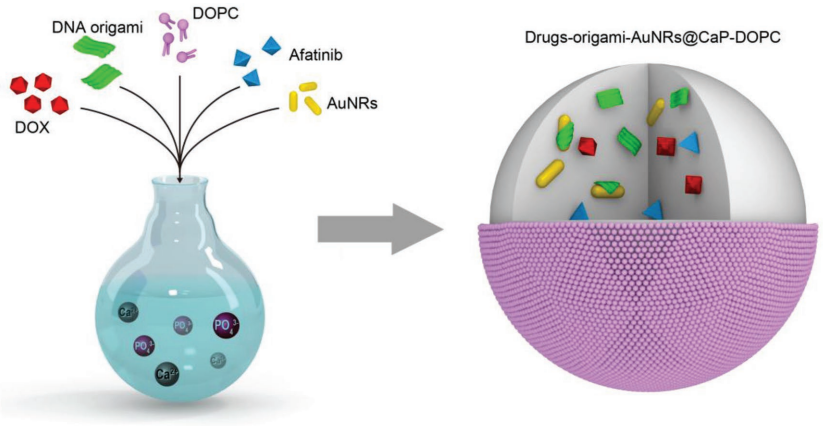

Scheme 1. The fabrication of $Ca_3(PO_4)_2$ nanoparticles incorporating anticancer drugs, DNA origami, AuNRs, and DOPC.

activation of the DNA origami hinder its biomedical applications.[6] Thus it is of great interest to protect DNA origami in a carrier and to evaluate the function of DNA origami in anticancer drug delivery.

To develop a comprehensive and biocompatible platform for biomedical applications, we select natural calcium phosphate [$Ca_3(PO_4)_2$], which we hypothesize to significantly improve the bioavailability of DNA origami and, in addition, to endow the nanocomposite with high drug loading capacity.[7] As a nontoxic delivery nanovehicle,[7] $Ca_3(PO_4)_2$ is relatively stable in the blood stream, but rapidly dissolves in the acidic pH around solid tumors.[7,8] $Ca_3(PO_4)_2$ can incorporate a broad variety of payloads due to the easily substituted matrix,[7] and its inherent structure enables efficient incorporation of nuclear acids and facilitates cellular uptake.[9] Another advantage of $Ca_3(PO_4)_2$ is the straightforward fabrication and payload encapsulation process achieved by mixing the different elements during the precipitation reaction.[7] Gold nanorods (AuNRs) have a photothermal responsive property and the potential to generate nanobubbles, and are therefore promising materials to enhance DNA origami and drugs permeation into the tumor.[10] AuNRs have also shown advantages in loading of nucleic acids and hydrophilic agents,[2] and they are hypothesized to enhance the DNA origami incorporation into $Ca_3(PO_4)_2$. Lipid coating is considered here to enhance the biocompatibility and minimize the aggregation of the nanocomposite.[11] The phospholipid, either as liposomes or coating materials, can reduce drug side effects and enhance the biocompatibility of the nanocomposite.[12]

Here, we have created a multifunctional nanocarrier with the biodegradable $Ca_3(PO_4)_2$ for incorporation of DNA origami, short AuNRs, and molecular targeted therapeutics. The hydrophilic drug (doxorubicin, DOX) and the hydrophobic molecular targeted drug (afatinib) with and without DNA origami are codelivered to create synergistic anticancer effects. A thin layer of 1,2-dioleoyl-*sn*-glycero-3-phosphocholine (DOPC) phospholipid is introduced onto the $Ca_3(PO_4)_2$ to reduce the potential adverse drug effects,[11b] to sustain the drug release and to minimize the aggregation of $Ca_3(PO_4)_2$ (**Scheme 1**).

2. Results and Discussion

2.1. Materials Characterization

The rectangular shaped DNA origami is soft and difficult to be delivered,[1c] and in this study it is synthesized to act as a model DNA origami for $Ca_3(PO_4)_2$ incorporation and for studying the synergistic effect between the DNA origami and the therapeutics (**Figure 1**A). As shown in Figure 1A, the DNA origami has a diameter of about 100 × 70 × 2 nm. Short AuNRs,[12] around 50 nm in length (Figure 1B,C), are synthesized to endow the nanoplatform with photothermal responsiveness.[12] $Ca_3(PO_4)_2$ particles are fabricated for simultaneous incorporation of drugs, AuNRs, and DNA origami using a one-step solvent free process. Hydrophilic (DOX, AuNRs, and DNA origami) and hydrophobic molecular targeted (afatinib) therapeutics are incorporated into $Ca_3(PO_4)_2$ particles using mechanical stirring. Scanning electron microscope (SEM) images show the different morphology of $Ca_3(PO_4)_2$ particles loaded with the different payloads (Figure 1D–I; Figure S1, Supporting Information). Energy-dispersive X-ray spectroscopy (EDX) analysis confirms the successful loading of AuNRs into $Ca_3(PO_4)_2$ since calcium, gold, and phosphate are detected in the spectrometry (Figure S2, Supporting Information). The SEM images suggest that the drugs and the AuNRs are mainly encapsulated within the $Ca_3(PO_4)_2$ particles instead of adsorbed on the surface, as shown in Figure 1E,F. By measuring the initial and final concentration of the drugs, the calculated loading efficiency is above 86%. Similarly, DOPC is incorporated either within or on the surface of the $Ca_3(PO_4)_2$ particles as indicated by the smooth surfaces of the particles form by mixing with DOPC, as shown in Figure 1G.

2.2. DNA Origami Encapsulation and Stability in $Ca_3(PO_4)_2$

DNA origami seems to be partially absorbed on the surface of $Ca_3(PO_4)_2$ particles as suggested by the very different morphology of the surface of the particles shown by the SEM image in Figure 1H. This presumably occurs because the DNA origami is very soft, with a 1 nm thickness, and can thus be easily folded on the surface of the particles (Figure 1H).[1c] The surface accumulation of DNA origami is essentially eliminated by addition of AuNRs and DOPC, as shown by the very smooth surfaces of the calcium phosphate particles prepared by mixing all component together as shown in Figure 1I. In addition, the incorporation rate of DNA origami inside $Ca_3(PO_4)_2$ increases from 73% to 94% in the presence of AuNRs.[13]

To evaluate the interaction between the AuNRs and the DNA origami, we mix AuNRs with DNA origami at high (10 ng mL^{-1}) and low AuNRs (1 ng mL^{-1}) concentrations. AFM image of DNA origami and gold nanorods interaction is shown in **Figure 2**A. Since gold nanorods have different height as DNA origami, the height is increased, so the DNA origami is not as clear as Figure 1A of DNA origami alone. After incubation for

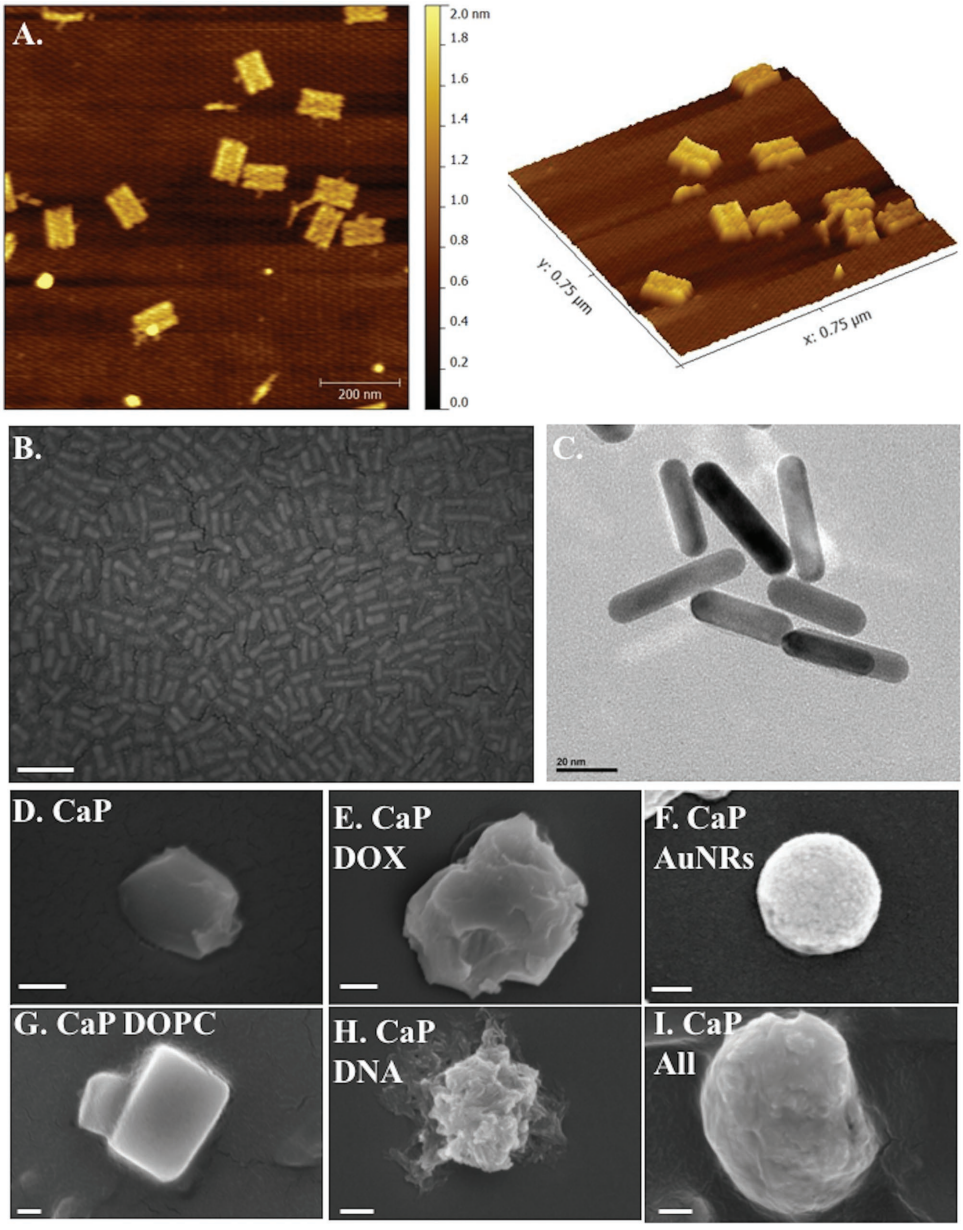

Figure 1. Morphology of the synthesized nanomaterials. A) AFM of DNA origami. B) SEM and C) TEM of AuNRs. SEM of D) $Ca_3(PO_4)_2$ nanoparticles and $Ca_3(PO_4)_2$ incorporating E) DOX, F) AuNRs, G) DOPC, H) DNA origami, and I) drugs/DNA origami/AuNRs and DOPC (CaP All). The scale bars denote 100 nm in (B) and (D–I).

1 h, the AuNRs are removed by centrifugation and the supernatants are analyzed with 0.8% agarose gel to measure the remaining concentration of free DNA origami. The DNA origami band is completely absent in the sample with 10 ng mL^{-1} AuNR whereas a very weak band is observed in the sample with 1 ng mL^{-1} AuNRs as shown in Figure 2B. The results confirm the strong interaction between AuNRs and DNA origami, and help explain how the AuNRs can improve the incorporation of the DNA origami within the calcium phosphate nanoparticles.

To test whether the DNA origami retains its structure during $Ca_3(PO_4)_2$ encapsulation, we dissolve $Ca_3(PO_4)_2$ at pH 5.0 to release the loaded DNA origami. Then the structural integrity of the DNA origami in $Ca_3(PO_4)_2$ is confirmed with a Förster resonance energy transfer (FRET) experiment (Figure S3, Supporting Information). Two fluorescent chromophores, TET (Em 535 nm) and TAMRA (Em 580 nm) are designed in the DNA origami structure at close connective positions through staple chains to create the FRET effect.[14] DNA origami shows different fluorescent pattern if there is a structural change in the nanostructure.[14] The DNA origami is released from the $Ca_3(PO_4)_2$ at pH 5.0 and has only a minor shift in the position of the fluorescent peaks as compared to those of the original DNA origami control; by contrast, pure DNA origami at pH 5.0 shows a totally different fluorescent pattern, as shown in Figure 2C. These results further demonstrate that $Ca_3(PO_4)_2$ encapsulation protects the DNA origami from degradation.

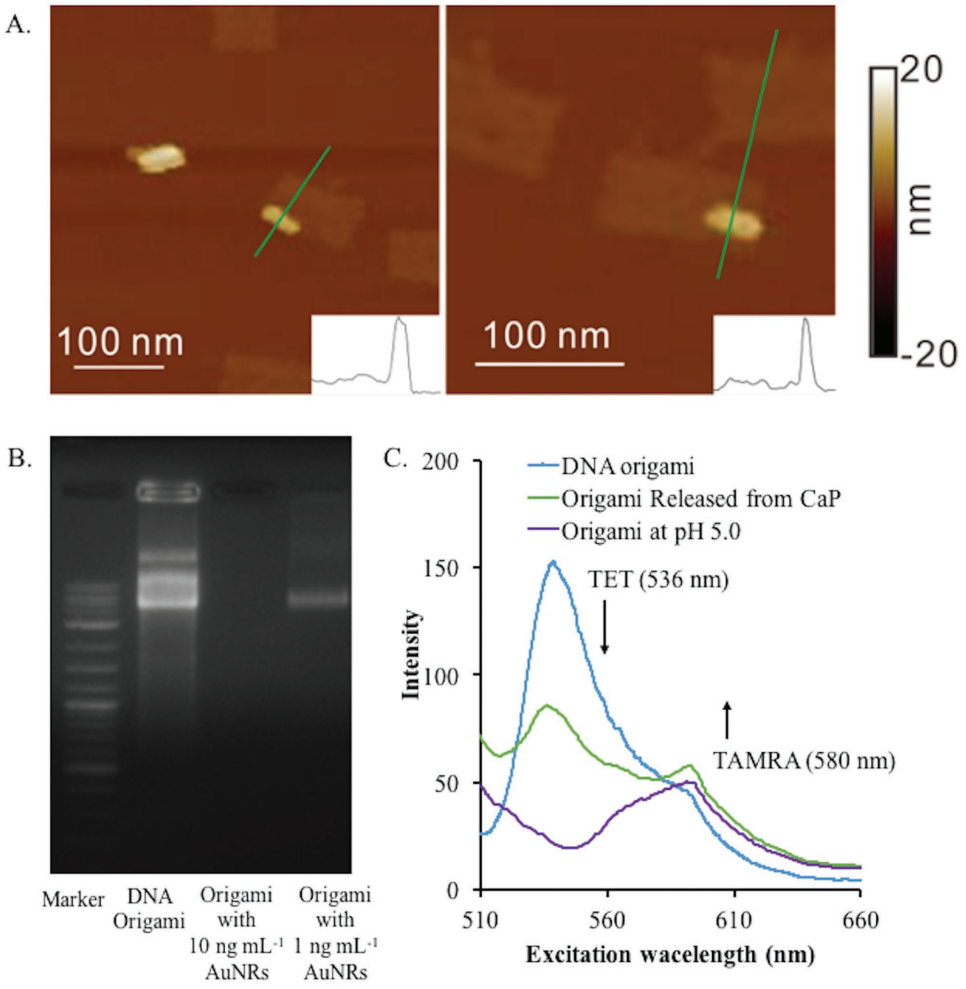

Figure 2. A) AFM images to show the AuNRs and DNA origami interaction. B) Agarose gel analysis of the interaction between DNA origami and AuNRs. 3 ng mL^{-1} DNA origami is incubated with 10 and 1 ng mL^{-1} of AuNRs and subsequently the AuNRs are removed and the free DNA origami in the supernatants is analyzed with agarose gel. C) FRET analysis of the protection of DNA origami by $Ca_3(PO4)_2$ in acidic conditions. TET (535 nm) and TAMRA (580 nm) are conjugated onto the DNA origami at close connected positions. The fluorescent patterns of pure DNA and DNA origami released from Ca3(PO4)2 at pH 5.0 are compared with pure DNA origami at pH 7.4.

2.3. Release of Different Contents

The release of therapeutics from calcium phosphate with and without DOPC coating is measured either by UV–vis spectrophotometry at 488 nm for DOX or 975 nm for AuNRs, or by high-performance liquid chromatography (HPLC) for afatinib. We calculate the drug encapsulation efficiency based on the measured DOX concentration at different ratios between the $CaCl_2/K_3PO_4$ at the same mechanical stirring rate (Table S1, Supporting Information). In vitro digestion study of DOX at different ratios between the hydrophilic and the hydrophobic drugs was performed at 37 °C (Table S2, Supporting Information). The hydrodynamic diameter of $Ca_3(PO_4)_2$ with and without drug loading before or after therapeutics release was measured by dynamic light scattering (DLS) measurement (Tables S3 and S4, Supporting Information). The encapsulation efficiency of AuNRs is above 95%. The loading of DNA origami is detected by microplate reader based on fluorescence intensity. The encapsulation efficiency of DNA origami is about 94% in the presence of AuNRs. In vitro release studies confirm that no initial burst release is observed and about 20–30% of the drugs, 15–25% of AuNRs, and 20–30% of DNA origami are released within 24 h from the $Ca_3(PO_4)_2$ nanoparticles in phosphate buffered saline (PBS) at pH 7.4 (**Figure 3**). With a DOPC layer, the drug release is sustained, as only 10–20% drugs are released within 24 h at pH 7.4 (Figure 3B). At pH 5.2, the majority of the drugs are burst released with the degradation of $Ca_3(PO_4)_2$ particles (Figure 3C,D).[7,8]

In addition to the pH responsiveness of the $Ca_3(PO_4)_2$, AuNRs endow the nanocomposite with heat and photothermal responsive property. The release rate of DOX is clearly faster at temperature of 45 °C than at 37 °C in the presence of AuNRs, while the drug release profile is similar at both temperatures without AuNRs (Figure 3E). Under laser irradiation at 656 nm excitation wavelength, the DOX release is ultrafast and the photothermal responsiveness is significant compared with thermal heating; for which 80% of the drug releases within 30 min of laser irradiation in the presence of AuNRs (Figure 3F). Since

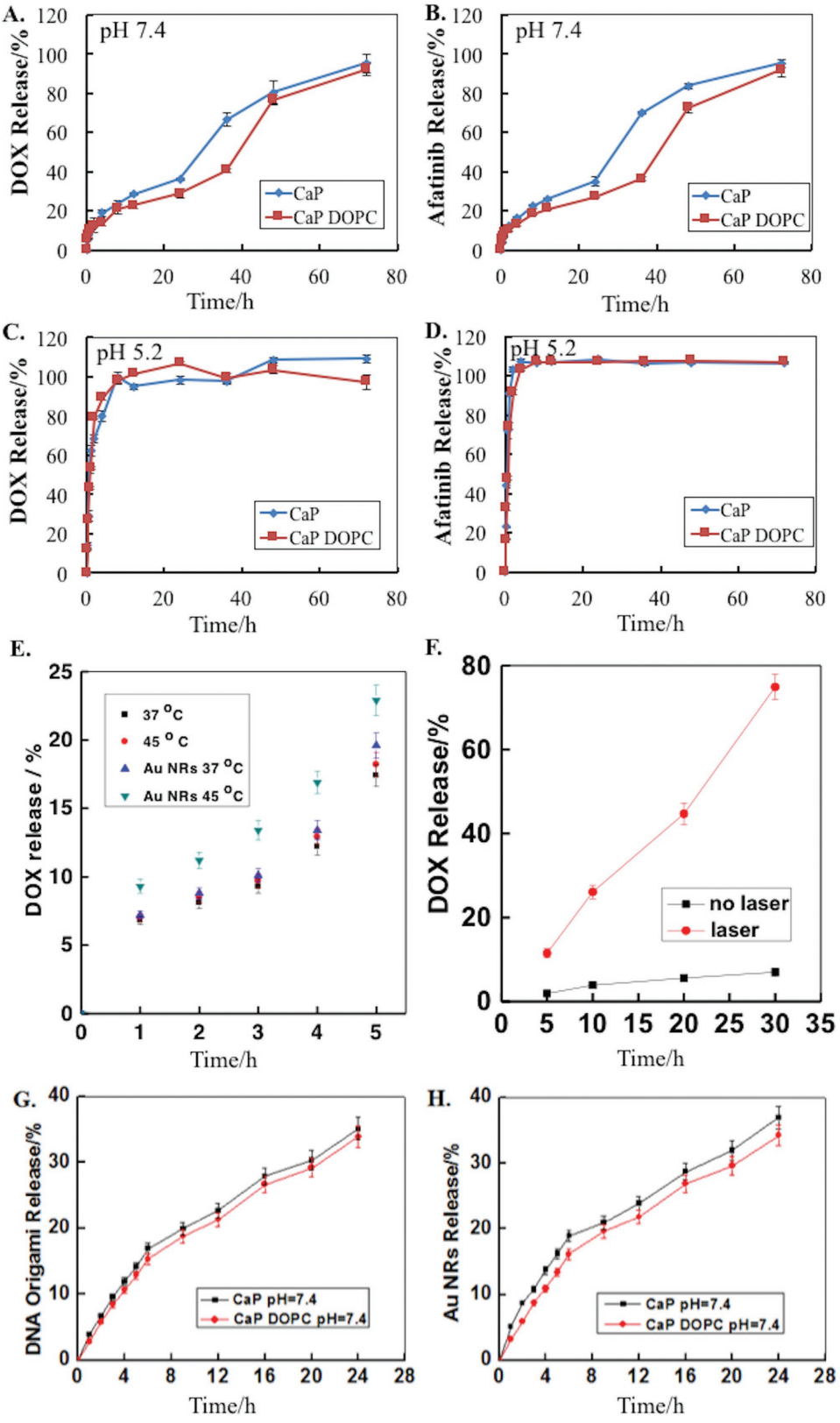

Figure 3. The pH, heat, and photothermal responsive drug release. A–D) DOX and afatinib release from $Ca_3(PO_4)_2$ with and without DOPC coating at pH 7.4 and pH 5.2. E) Heat responsive DOX release from $Ca_3(PO_4)_2$@DOPC at 37 and 45 °C. F) Laser-induced DOX release from AuNRs@$Ca_3(PO_4)_2$@DOPC by irradiation under laser for different time intervals. G) DNA origami releases from $Ca_3(PO_4)_2$ with and without DOPC coating at pH 7.4. H) AuNR releases from $Ca_3(PO_4)_2$ with and without DOPC coating at pH 7.4. All data represent mean ± S.D. ($n = 3$).

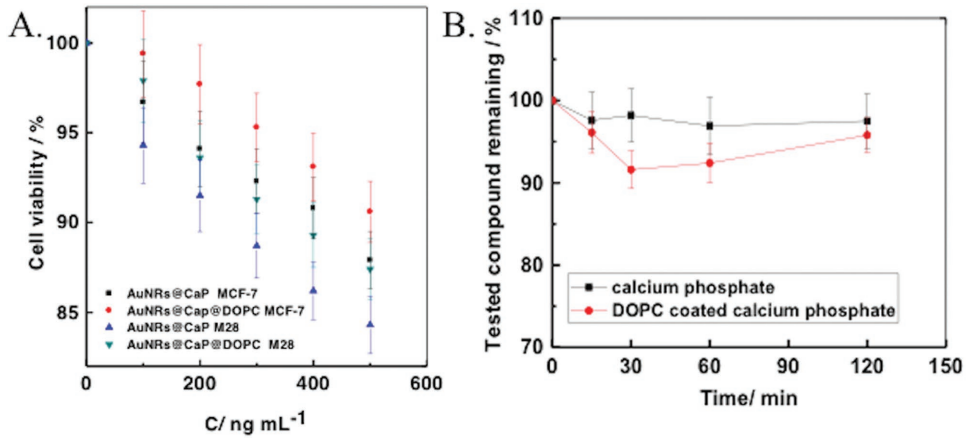

Figure 4. A) The cell viability of MCF-7 and M28 cells treated with AuNRs and DNA origami coloaded $Ca_3(PO_4)_2$ nanoparticles with and without DOPC coating after 24 h incubation at 37 °C. B) The plasma stability of afatinib in the $Ca_3(PO_4)_2$ particles coated with and without phospholipid DOPC. The percentage of parent compound remaining after incubation in human plasma is plotted versus incubation time. All incubations are performed in triplicates using 96-well cell culture plate. All data represent mean ± S.D. (n = 3).

photothermal responsiveness is affected by laser power and amount of AuNRs, it is possible to tailor the drug release profiles by adjusting those parameters. In addition, the incorporation of AuNRs into the biodegradable $Ca_3(PO_4)_2$@DOPC nanocomposite provides potential photothermal therapy for effective cancer treatment.

2.4. Biocompatibility and Plasma Stability

It is well-known that DOX is highly toxic to both endothelial and cardiomyocytes cells, which accounts for severe side effects upon systemic administration.[15] The same problem is associated with many other chemotherapy drugs. Thus, biocompatible carriers are needed for delivery of those drugs to hinder the side effects. The cell cytotoxicity of the $Ca_3(PO_4)_2$ loaded with AuNRs and DNA origami is evaluated in MCF-7 (breast cancer cells) and M28 (normal human cells) using a live/dead assay (**Figure 4**A). The $Ca_3(PO_4)_2$ nanoparticles with and without DOPC coating do not show visible toxicity, as 90% of the MCF-7 and M28 cells survive in the presence of 400 μg mL^{-1} of $Ca_3(PO_4)_2$. DOPC further improves the biocompatibility of the $Ca_3(PO_4)_2$ toward both cancer cells and normal human M28 cells. This demonstrates that the synthesized $Ca_3(PO_4)_2$@DOPC is highly biocompatible and suitable for drug delivery.

We also carry out a human plasma stability assay to determine whether afatinib leaks out from the AuNR@$Ca_3(PCO_4)_2$@DOPC using the standard human plasma stability protocol (Figure 4B). After 120 min, the remaining afatinib in AuNR@$Ca_3(PCO_4)_2$ is 95% and 93% without and with DOPC coating, respectively. This confirms the stability of afatinib loaded AuNR@$Ca_3(PCO_4)_2$@DOPC particles, which shows potential for in vivo translation.

2.5. Therapeutically Synergistic Effects

The synergistic effect of DNA origami and drug combination in $Ca_3(PO_4)_2$@DOPC toward MCF-7 cells is shown in **Figure 5**A. The drug combination is more efficient in killing the cancer cells than that of single drug at the same concentration. This indicates the synergistic killing effect of the drug combination. DNA origami further enhances the cancer cells apoptosis together with single drug or drug combination, and thus exhibits synergism with drugs.

We calculate the combination index of different drugs after incubation with human epidermal growth factor receptor 2 (HER2) positive breast cancer cell (SKBR-3) and HER2 negative breast cancer cell (MCF-7), which can indicate the type and amount of interaction between the two drugs with respect to the different cells.[16] As shown in Figure 5B, the combination of DOX and afatinib has a stronger synergistic effect for killing SKBR-3 cells than for MCF-7 cells. SKBR3 cells overexpress HER2, and afatinib is a small molecular target drug for HER2.[17] The selective targeted killing of HER2 positive cancer cells suggests the potential of designing a targeted nanocomposite by loading different drug combinations with and without DNA origami into the $Ca_3(PO_4)_2$@DOPC.

Multidrug resistance is one of the greatest challenges in cancer treatment. To investigate the enhanced inhibition of multidrug resistance, we study the in vitro cell viability of AuNRs@$Ca_3(PO_4)_2$@DOPC loaded DOX, afatinib, DNA origami, and their combinations toward DOX resistant breast cancer (MCF-7/DOX) cells. As shown in Figure 5C, free DOX exhibits a rather low cytotoxicity on MCF-7/DOX cells, which indicates that the cells have a high drug resistance to DOX molecules. Multidrug loaded AuNRs@$Ca_3(PO_4)_2$@DOPC exhibits a much stronger cytotoxicity on MCF-7/DOX cells. A remarkable inhibition against multidrug resistant is observed for drugs coloaded with DNA origami as compared to any single drug and drug combination without DNA origami. The results demonstrate the synergistic effect between DNA origami and drugs on effective inhibition of multidrug resistance. DNA origami contributes to the enhancement of cancer drugs on inducing MCF-7/DOX death of cells.

To evaluate the laser-induced cancer cell death, we incubate the MCF-7/DOX cells with $Ca_3(PO_4)_2$@DOPC particles loaded with DOX, coloaded with DOX/AuNRs, and coloaded

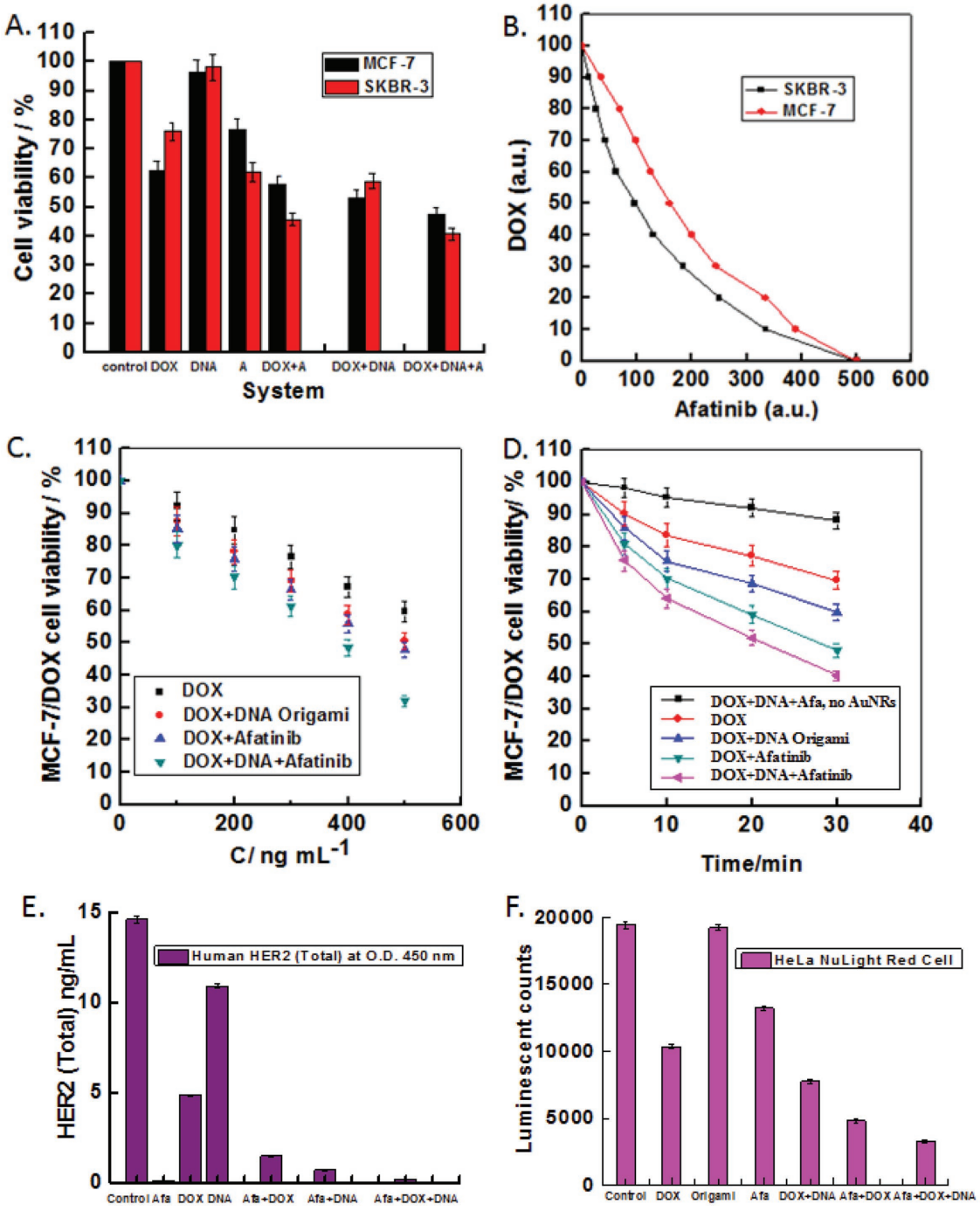

Figure 5. The synergism effects of DNA origami and drugs. A) The synergistic killing effect of DOX, afatinib (and DNA origami coloaded AuNRs@$Ca_3(PO_4)_2$@DOPC nanoparticles at different drugs concentrations in MCF-7 and SKBR-3 cells after 24 h incubation at 37 °C using a live/dead assay. The total concentration of drugs is 360 ng mL^{-1}, $C_{DOX}/C_{afatinib}$ = 2:1, and 10 ng mL^{-1} AuNRs and 3 ng mL^{-1} of DNA origami are coloaded. B) The isobologram of the DOX+afatinib combination on killing SKBR-3 and MCF-7 cells. C) The multidrug resistance inhibition by the drugs-loaded and DNA origami coloaded AuNRs@ $Ca_3(PO_4)_2$@DOPC nanoparticles on MCF-7/DOX cells after 24 h incubation at 37 °C. D) Laser induced cancer cell killing. The total drug concentration is 360 ng mL^{-1} ($C_{DOX}/C_{afatinib}$ = 2:1), 10 ng mL^{-1} AuNRs is added in all samples, except in the DOX+DNA+afatinib no AuNR control. 3 ng mL^{-1} of DNA origami is included to generate synergism. All samples are incubated with MCF-7/DOX cells under laser irradiation at 656 nm at different time intervals from 5 to 30 min. The cell viability is measured after 2 h of the laser irradiation using a live/dead assay. All data represent mean ± S.D. (n = 3). E) HER2 (Total) ELISA kit for measurement of HER2 protein at optical density 450 nm on SKBR3 cells. The total drug concentration is 12 µg mL^{-1}, $C_{DOX}/C_{afatinib}$ = 2:1, DNA origami is 3 ng mL^{-1}, AuNR is 10 ng mL^{-1}, AuNRs@$Ca_3(PO_4)_2$@DOPC without drugs, and DNA origami is set as control. All data represent mean ± S.D. (n = 3). F) ATP-based variability assay on HeLa cells. The total drug concentration is 12 µg mL^{-1}; $C_{DOX}/C_{afatinib}$ = 2:1, DNA origami is 3 ng mL^{-1}, AuNR is 10 ng mL^{-1}, and AuNRs@ $Ca_3(PO_4)_2$@DOPC is set up as control. All data represent mean ± S.D. (n = 3).

with DOX/AuNRs/DNA origami, each under laser irradiation of 5, 10, 20, and 30 min (Figure 5D). The laser power used in the experiment is tolerable for the cells, since only minor toxicity is observed for $Ca_3(PO_4)_2$@DOPC particles coloaded with drugs and DNA origami without AuNRs under laser irradiation. By contrast, in the presence of AuNRs, the drug loaded $Ca_3(PO_4)_2$@DOPC immediately starts to kill the MCF-7/DOX cells (Figure 5D). This is due to the photothermal responsive drug release and hyperthermic effect of AuNRs to MCF-7/DOX cells. Interestingly, DNA origami acts synergistically with AuNRs and drugs on inducing the killing of the MCF-7/DOX cells under laser irradiation. The DOX/AuNRs/DNA origami coloaded $Ca_3(PO_4)_2$@DOPC shows the strongest killing effect on MCF-7/DOX cells under laser irradiation (Figure 5D).

To study the HER2 positive cells' targeted killing, we perform a Human HER2 ELISA assay to detect and quantify the full-length HER2 protein from human HER2 positive SKBR3 breast cancer cells' lysates treated by the drug and drugs combination with and without DNA origami loaded in AuNR@ $Ca_3(PCO_4)_2$@DOPC for 6 h. Figure 5E shows that HER2/EGFR targeted afatinib has high HER2 targeted killing and dramatically reduces HER2 expression. This is because this molecular targeted drug is a protein kinase inhibitor that irreversibly inhibits HER2 protein and targets HER2 positive cancer cells.[17] DNA origami enhances the HER2 selectively targeted killing when combined with afatinib, which also confirms the synergism between DNA origami and afatinib.

We also perform a Human HER2 (pY1248) ELISA assay to detect and quantify the phosphorylated HER2(pY1248) protein from lysates of human HER2 positive SKBR3 breast cancer cells. Figure S4 (Supporting Information) shows that afatinib can also effectively reduce HER2 (pY1248) expression either alone or when combined with other therapeutics. DNA origami promotes the inhibition of HER2 (pY1248) expression and again shows a synergistic effect with drugs.

To evaluate the enhancement on HeLa NuLight Red cell death induced by drug combinations with and without DNA origami, we perform a luminescent ATP detection cytotoxicity assay at 37 °C. Figure 5F shows that the DNA origami enhances the cytotoxicity on HeLa cells by combining with either single drugs or drug combinations, which is additional evidence for the synergism between DNA origami and drug/drugs combination. The main function of DNA origami is its synergistic effects with anticancer drugs to promote apoptosis of cancer cells. We discussed in detail the function of DNA origami in our previous work.[12c] In this work, DNA origami has the same function to promote cancer cells apoptosis through synergism.

3. Conclusion

In summary, we fabricate DNA origami, AuNRs, and simultaneously incorporate them with molecular targeted anticancer drugs into $Ca_3(PO_4)_2$ nanoparticles coated with phospholipid DOPC. The established biodegradable nanocomposite shows very good biocompatibility and high drug loading capacity. The $Ca_3(PO_4)_2$ and AuNRs endow the platform with pH and photothermal responsiveness. DNA origami is successfully incorporated into the AuNRs@ $Ca_3(PO_4)_2$@DOPC without disrupting the DNA origami structure, and the nanocomposite protects the DNA origami from an acidic environment. Moreover, the DNA origami and drug combination work synergistically to enhance the therapeutic effectiveness and suppress multidrug resistance in MCF-7/DOX cells. This combination also induces apoptosis of HeLa cells and enhances the targeted killing of HER2 positive SKBR-3 cells. The addition of AuNRs induces hyperthermic cancer cell killing on MCF-7/DOX cells and the DNA origami further enhances this effect. Overall, the multifunctional DNA origami based AuNRs@$Ca_3(PO_4)_2$@DOPC nanocomposite can be easily formulated at low cost with high yield, and can load multiple drugs at high loading. It can also protect DNA origami from degradation and create synergism through codelivery of DNA origami and drugs. Thus, the nanocomposite has great potential for advanced biomedical applications.

4. Experimental Section

Materials: Doxorubicin hydrochloride (DOX), afatinib, Erlotinib, and Docetaxel were purchased from LC Laboratories with purity >99.0%. DOPC was purchased from Avanti Polar Lipid in powder form. Calcium chloride, Na_3PO_4, $HAuCl_4$, $NaBH_4$, ascorbic acid, and cetrimonium bromide (CTAB) were purchased from Sigma-Aldrich and used without further purification. PBS (1×) without calcium or magnesium was purchased from Lonza. M28, SKBR-3, and MCF-7 cell lines were purchased from ATCC. Live/dead assay kit was purchased from Life technologies. Highly purified distilled water was obtained from a Millipore Milli-Q system. All solutions were filtered by a 0.2 µm membrane (Anodisc) prior to the experiments.

Synthesis of $Ca_3(PO_4)_2$ with and without DOPC Coating: The $Ca_3(PO_4)_2$ nanoparticles were synthesized by adding 1 mL of 1 M $CaCl_2$ solution into 1.3 mL of 1 M Na_3PO_4 and magnetic stirred at 1600 rpm for 10 min. Then, 5 mL of pure water was added into the reactant and formed a suspension. The suspension was centrifuged at 14400 rpm for 15 min to collect the formed calcium phosphate nanoparticles in pellet.

100 mg mL^{-1} DOPC in ethanol solution was subsequently dropped into the $Ca_3(PO_4)_2$ reaction solution with magnetic stirring at 600 rpm for 10 min. Then DOPC hybrid $Ca_3(PO_4)_2$ nanoparticles were collected by centrifugation at 16 100 rpm for 15 min, following the same procedure as mentioned above.

Synthesis of DNA Origami: Single stranded M13mp18 DNA (7249 nucleotides) was mixed with a ten times molar ratio of staple strands in buffer (40×10^{-3} M tris, 20×10^{-3} M acetic acid, 2×10^{-3} M EDTA, and 12.5×10^{-3} M magnesium acetate, pH 8.0). The 2D rectangle shape DNA was synthesized in aqueous solution by special sequence oligonucleotides following the previous protocol.[18]

Synthesis of AuNRs: AuNRs were synthesized by seed-mediated growth according to the previous described procedure.[1] CTAB was used as stabilizer. The morphology of the AuNRs was determined by transmission electron microscope (TEM) and SEM. The AuNR-CTAB was washed twice with Milli-Q water and centrifuged at 16 100 rpm for 15 min to remove the excess of reactants. The AuNRs concentration was determined by the UV–vis spectrum (Cary 100 UV–vis spectrophotometer, Agilent Technologies) with known extinction coefficients. The AuNRs concentration in the experiments used was from 1 to 20 ng mL^{-1}.

Incorporation of AuNRs, DNA Origami and Multiple Drugs into the $Ca_3(PO_4)_2$ Nanoparticles: Incorporation of the AuNRs, DNA origami, anticancer drug DOX, and afatinib into the photothermal responsive $Ca_3(PO_4)_2$ hybrid nanoparticles coated with and without DOPC was conducted by the following procedure. 1 mL of 1 M of $CaCl_2$ and

100 µL of DOX (10 mg mL^{-1}) + 100 µL of 20 ng mL^{-1} AuNRs + 100 µL of 6 ng mL^{-1} origami DNA were gently mixed for 10 min at 800 rpm with a magnetic stirring, and then 0.4 mL of afatinib (1.25 mg mL^{-1} in ethanol) and 1 mL of 1 M of Na_3PO_4 were added and magnetic stirred at 1600 rpm for 10 min. Subsequently, 100 mg mL^{-1} DOPC in ethanol solution was dropped into the $Ca_3(PO_4)_2$ reaction solution. After reaction, 5 mL of pure water was added to the mixture and kept for 2 h, the sedimented large particles in bottom were discarded, and the suspension was centrifuged at 16 100 rpm for 15 min to collect the nanoparticles. The amount of DOX in the supernatant and the precipitate was measured using a UV–vis spectrophotometer (ND-1000 Nanodrop) at 234 nm. Different molar ratios of $CaCl_2/Na_3PO_4$ were tested (1:1.3, 1:1.2, 1:1.1, 1:1, 1.1:1, and 1.2:1) in order to achieve the highest incorporation rate (Table S1, Supporting Information). The highest ratio of 1:1.3 was found to be optimal and selected in all the following studies.

Characterization of the Hybrid Hanoparticles with and without Payloads: The morphology of the $Ca_3(PO_4)_2$ nanoparticles, DOX@$Ca_3(PO_4)_2$, AuNRs@$Ca_3(PO_4)_2$, origami@$Ca_3(PO_4)_2$, DOPC-coated $Ca_3(PO_4)_2$, and DOX/origami/AuNRs@$Ca_3(PO_4)_2$@DOPC were evaluated by SEM (Zeiss EVO) at room temperature. The elements of the $Ca_3(PO_4)_2$ nanoparticles, AuNRs@$Ca_3(PO_4)_2$, and DOPC-coated $Ca_3(PO_4)_2$ nanoparticles were evaluated by SEM-EDX (Zeiss Supra 55) at room temperature.

FRET Analysis: Two fluorescent chromophores, TET (Em 535 nm) and TAMRA (Em 580 nm) were conjugated to the rectangle DNA origami in connected positions following the previous protocol (position 1: 91-TET and 89-TAMRA).[18] Due to the resonance energy transfer effect, TAMRA peak at 580 nm was quenched by TET peak; and the TET peak at 535 nm would be stimulated. Upon the degradation of the DNA origami structure, the TAMRA would be separated from TET, and a peak at 580 nm would be observed. The fluorescent chromatography was acquired from F-7000 fluorescence spectrometer (Hitachi, Tokyo, Japan) at excitation of 473 nm.

In Vitro Release of the Therapeutics and Photothermal Effect of AuNRs: The in vitro release of the anticancer drugs DOX and afatinib from the $Ca_3(PO_4)_2$ nanoparticles coated with and without DOPC were evaluated by a dynamic dialysis method using dialysis bag. Aliquots of each drug-loaded suspensions in 1 mL of PBS was placed in mini dialysis bag (2 mL, MWCO 8 kDa cutoff; GE Health, USA) and floated in 100 mL pH 7.4 PBS release medium or pH 5.2 buffer and maintained at 37 °C with a paddle revolution speed of 100 rpm using G24 Environmental incubator shaker (New Brunswick Scientific Co. Inc. USA). At certain interval times, 500 µL of the released sample was withdrawn and 500 µL of fresh medium was added to the bulk solution to keep the volume of the solution constant. The DNA origami and AuNRs release was studied without using dialysis bag to avoid the blocking of the materials in the bag. The concentration of afatinib from the released sample was analyzed by HPLC at UV absorbance of 260 nm. The concentration of DOX was measured either by HPLC at UV 488 nm or calculated from the maximum peak at 488 nm with UV–vis spectrophotometer (Agilent Cary 1100). The concentration of DNA origami released from the $Ca_3(PO_4)_2$ was analyzed by Synergy H1 Multi-Mode Microplate Reader (BioTek Instruments, Inc.USA). The origami was labeled by SYBR Green I. The AuNRs concentration was determined from the UV–vis spectrum (Cary Agilent 1100) at 975 nm.

The heat responsive drug release was performed at 45 °C with and without 10×10^{-3} M AuNRs. Laser-induced photothermal responsive drug release was performed under laser irradiation (6 W cm^{-2}) at wavelengths of 656 nm for 5, 10, 20, and 30 min. The release of DOX from $Ca_3(PO_4)_2$ nanoparticles was measured and calculated by nanodrop spectrophotometer (ND-1000 nanodrop) at a maximum UV absorbance of 234 nm and the release of AuNRs was monitored with UV–vis spectrum (Cary Agilent 1100) at a maximum absorbance of 975 nm.

HPLC Analysis: The concentration of afatinib from the released samples at different time intervals and the residue samples was analyzed by injecting 20 µL of each sample into an Agilent 1200 HPLC system. The separation was carried out using an Agilent ZORBAX Eclipse Plus C18 column (4.6 × 150 mm). The separation was performed with a flow rate of 1 mL min^{-1} with mobile phases of acetonitrile and 0.1% trifluoroacetic acid.

Cell Viability Evaluation: MCF-7 (a human breast cancer cell line) and M28 (a human mesothelioma cell line) were maintained in Dulbecco's modified Eagle's medium supplemented with 10% heat-inactivated fetal bovine serum and 1% penicillin–streptomycin. At 80% cell confluency, MCF-7 or M28 cells were collected and seeded on 96-well plates (1.0×10^4 cells per well) in 100 µL cell medium. Then 100 µL of medium containing 1×10^{-6} M calcein AM + 2×10^{-6} M of ethidium homodimer-1 (EthD-1) was added to each well. DNA origami/AuNRs@$Ca_3(PO_4)_2$ with and without DOPC coating were added to different wells at different concentrations (10, 50, and 100 µg mL^{-1}) and incubated with cells for 24 h in an atmosphere of 5% CO_2. The cell number and density was counted using an Invitrogen Countess automated cell counter. The fluorescence intensity was measured at the excitation wavelengths of 488 and 544 nm for calcein AM and EthD-1, respectively, and the emission wavelengths of 530 and 610 nm for calcein AM and EthD-1, respectively, using a microplate reader SpectraMax i3 (Molecular device). The cell viabilities of $Ca_3(PO_4)_2$ nanoplatform on MCF-7 or M28 cell lines were calculated according to live/dead assay, as described in the previous work.[12b]

In Vitro Cytotoxicity Studies: MCF-7 and SKBR-3 (HER2 positive breast cancer cell line) were seeded on 96-well plates as described above. DOX, DNA origami, afatinib, DOX+DNA origami, DOX+afatinib, and DOX+DNA origami+afatinib were loaded into AuNRs@$Ca_3(PO_4)_2$@DOPC and incubated with the two cells at different concentrations. The cell viability was calculated according to live/dead assay using AuNRs@$Ca_3(PO_4)_2$@DOPC as control.

Human Plasma Stability Study: Incubations of Afatinib incorporated calcium phosphate coated with and without DOPC were carried out in 96-well cell culture plate (Corning) in five aliquots of 100 µL each (one for each time point). Test compounds (10×10^{-6} M, final solvent concentration 1%) and DMSO (10×10^{-3} M, final concentration 2.5%) were incubated at 37 °C. Five time points over 120 min were analyzed (0, 15, 30, 60, and 120 min). All incubations were performed in duplicates. The samples were analyzed by HPLC-MS (API3000, AB Sciex). The percentage of parent compound remaining after incubation in human plasma was plotted versus incubation time.

The Synergistic Effect of Drugs Combination: The Isobologram was measured according to the therapeutics combination synergism theory according to the previous work.[12b] Abscissa and ordinate units were the concentrations of drugs afatinib and DOX on inhibiting MCF-7 cells and SKBR-3 cells; the drug afatinib had an IC_{50} (concentration giving 50% inhibition) of 500 a.u. (abscissa units), DOX had IC_{50} of 100 a.u (ordinate units).

Multidrug Resistance Test: DOX, DOX+DNA origami, DOX+afatinib, DOX+afatinib+DNA origami loaded AuNRs@$Ca_3(PO_4)_2$@DOPC were incubated with DOX resistant MCF-7/DOX cells and the cell viabilities were analyzed using the live/dead assay as described above.

Photothermal Responsive Cancer Cell Killing: The DOX and DOX+DNA origami loaded AuNRs@$Ca_3(PO_4)_2$@DOPC were incubated with MCF-7/DOX cells under laser irradiation (6 W cm^{-2}) at wavelengths of 656 nm for 5, 10, 20, and 30 min. The MCF-7/DOX cells incubated with DOX loaded $Ca_3(PO_4)_2$@DOPC without AuNRs were used as control. The cell viability was measured after 2 h of the laser irradiation using the live/dead assay as described above.

Human HER2 (Total) ELISA Assay: Invitrogen Human HER2 (Total) ELISA Kit (KHO0701) was used to detect and quantify the full-length HER2 protein independent of its phosphorylation state from SKBRS lysates treated with different therapeutics. SKBRS cells with density of 10^7 mL^{-1} were seeded on 12-well cell culture plate and treated with different therapeutics for 6 h. The optical density at 450 nm of the standards and samples according to the assay kit standard protocol was obtained using microplate reader (SpectraMax i3 from Molecular device).

Human HER2 (pY1248) ELISA Assay: Human HER2 (pY1248) ELISA assay was used to detect and quantify the phosphorylated HER2

(pY1248) protein of its phosphorylation state from SKBRS lysates treated with different therapeutics with and without DNA origami. SKBRS cells with density of 10^7 mL^{-1} were seeded on 12-well cell culture plate and treated with different therapeutics for 16 h. The optical density at 450 nm of the standards and samples according to the assay kit standard protocol was obtained using microplate reader (SpectraMax i3 from Molecular device).

ATP Detection Cytotoxicity on HeLa Cells: ATP Determination Kit (A22066) from Life Technologies was used to detect the bioluminescent at 560 nm for quantitative determination of ATP-based cytotoxicity of Hela cells after 4 h treatment of different therapeutics according to standard assay protocol. Hela cells with density of (1–1.2) $\times$ 10^4 cells per well were seeded on 96-well cell culture plates, allowed to adhere and treated for 4 h with different therapeutics (various concentration). After treatment, HeLa cells were exposed to the ATP standard reaction solution, and the luminescent intensity was measured on a luminescent microplate reader (SpectraMax L; Molecular device) at 560 nm emission wavelength. Mean and standard deviation was plotted for triplicates from each condition.

Statistical Analyses: All data represent mean $\pm$ S.D. (n = 3). The data were analyzed by a Student's t-test using the online version of GraphPrism software. The significance was set at probabilities of $^*p < 0.05$, $^{**}p < 0.01$, and $^{***}p < 0.001$, $n = 6$.

Supporting Information

Supporting Information is available from the Wiley Online Library or from the author.

Acknowledgements

H.Z., X.Q., H.C., and H.K. contributed equally to this work. The authors are grateful to the Fundamental Research Funds for the Central Universities (Grant No. FRF-BR-09-021B), 863 program of P. R. China (Grant No. 2006AA03Z108), NSF (Grant No. DMR-1310266), and Harvard MRSEC (Grant No. DMR-0820484) for financial support. H.Z. acknowledges Jane and Aatos Erkko Foundation (Grant No. 4704010) and the Academy of Finland (Grant No. 297580) for financial support. H.A.S. acknowledges the Academy of Finland (Grant Nos. 252215 and 281300), the University of Helsinki Research Funds, Biocentrum Helsinki, and the European Research Council (Grant No. 310892) for support. H.C. acknowledges the financial support from the National Natural Science Foundation of China (Grant No. 21005066). X.Q. and H.P. acknowledge Shanghai Pujiang Talent Project (15PJ1401800 and 16PJ1402700). The authors thank the Harvard CNS and FAS centers for providing the facilities for the cell experiments, AFM, TEM, FT-IR, DLS, SEM, and HPLC measurements. The authors acknowledge Prof. Nadrian Seeman for providing the origami DNA. The authors thank Dr. Arthur McClelland at Harvard CNS for helping with the laser irradiation experiment and David Lange at Harvard CNS for helping with the SEM-EDX measurements.

Conflict of Interest

The authors declare no conflict of interest.

Keywords

calcium phosphate, cancer treatment, DNA origami, gold nanorods, biomedical applications

Received: May 26, 2017
Revised: July 24, 2017
Published online:

[1] a) N. R. Jabir, S. Tabrez, G. M. Ashraf, S. Shakil, G. A. Damanhouri, M. A. Kamal, *Int. J. Nanomed.* **2012**, *7*, 4391; b) P. W. Rothemund, *Nature* **2006**, *440*, 297; c) Y.-J. Chen, B. Groves, R. A. Muscat, G. Seelig, *Nat. Nanotechnol.* **2015**, *10*, 748; d) N. Kolishetti, S. Dhar, P. M. Valencia, L. Q. Lin, R. Karnik, S. J. Lippard, R. Langer, O. C. Farokhzad, *Proc. Natl. Acad. Sci. USA* **2010**, *107*, 17939.
[2] V. P. Torchilin, *Adv. Drug Delivery Rev.* **2006**, *58*, 1532.
[3] Q. Zhang, Q. Jiang, N. Li, L. Dai, Q. Liu, L. Song, J. Wang, Y. Li, J. Tian, B. Ding, Y. Du, *ACS Nano* **2014**, *8*, 6633.
[4] Z. G. Wang, C. Song, B. Ding, *Small* **2013**, *9*, 2210.
[5] J. Liu, Z. Cao, Y. Lu, *Chem. Rev.* **2009**, *109*, 1948.
[6] S. D. Perrault, W. M. Shih, *ACS Nano* **2014**, *8*, 5132.
[7] M. Kester, Y. Heakal, T. Fox, A. Sharma, G. P. Robertson, T. T. Morgan, E. I. Altinoglu, A. Tabakovic, M. R. Parette, S. M. Rouse, V. Ruiz-Velasco, J. H. Adair, *Nano Lett.* **2008**, *8*, 4116.
[8] B. M. Barth, R. Sharma, E. İ. Altınoğlu, T. T. Morgan, S. S. Shanmugavelandy, J. M. Kaiser, C. McGovern, G. L. Matters, J. P. Smith, M. Kester, J. H. Adair, *ACS Nano* **2010**, *4*, 1279.
[9] A. Maitra, *Expert Rev. Mol. Diagn.* **2005**, *5*, 893.
[10] E. Y. Lukianova-Hleb, X. Ren, R. R. Sawant, X. Wu, V. P. Torchilin, D. O. Lapotko, *Nat. Med.* **2014**, *20*, 778.
[11] a) M. T. Haynes, L. Huang, *Adv. Genet.* **2014**, *88*, 205; b) S. Jain, S. R. Patil, N. K. Swarnakar, A. K. Agrawal, *Mol. Pharm.* **2012**, *9*, 2626.
[12] a) L. Vigderman, B. P. Khanal, E. R. Zubarev, *Adv. Mater.* **2012**, *24*, 4811; b) F. Kong, X. Zhang, H. Zhang, X. Qu, D. Chen, M. Servos, E. Mäkilä, J. Salonen, H. A. Santos, M. Hai, D. A. Weitz, *Adv. Funct. Mater.* **2015**, *25*, 3330; c) F. Kong, H. Zhang, X. Qu, X. Zhang, D. Chen, R. Ding, E. Mäkilä, J. Salonen, H. Santos, M. Hai, *Adv. Mater.* **2016**, *28*, 10195; d) F. Kong, H. Zhang, X. Zhang, D. Liu, D. Chen, W. Zhang, L. Zhang, H. Santos, M. Hai, *Adv. Funct. Mater.* **2016**, *26*, 6158.
[13] T. Zhang, N. Gao, S. Li, M. J. Lang, Q.-H. Xu, *J. Phys. Chem. Lett.* **2015**, *6*, 2043.
[14] K.-h. Yea, S. Lee, J. Choo, C.-H. Oh, S. Lee, *Chem. Commun.* **2006**, 1509.
[15] W. G. Kaelin Jr., *Nat. Rev. Cancer* **2005**, *5*, 689.
[16] W. R. Greco, G. Bravo, J. C. Parsons, *Pharmacol. Rev.* **1995**, *47*, 331.
[17] a) V. A. Miller, V. Hirsh, J. Cadranel, Y.-M. Chen, K. Park, S.-W. Kim, C. Zhou, W.-C. Su, M. Wang, Y. Sun, D. S. Heo, L. Crino, E.-H. Tan, T.-Y. Chao, M. Shahidi, X. J. Cong, R. M. Lorence, J. C.-H. Yang, *Lancet Oncol.* **2012**, *13*, 528; b) J. C. Singh, K. Jhaveri, F. J. Esteva, *Br. J. Cancer* **2014**, *111*, 1888.
[18] X. Wei, J. Nangreave, S. Jiang, H. Yan, Y. Liu, *J. Am. Chem. Soc.* **2013**, *135*, 6165.

